

**MEASUREMENT OF HIGH VOLTAGE USING RUTHERFORD
BACKSCATTERING SPECTROMETRY**

A Thesis

by

CELESTINO PETE ABREGO

Submitted to the Office of Graduate Studies of
Texas A&M University
in partial fulfillment of the requirements for the degree of

MASTER OF SCIENCE

December 2006

Major Subject: Nuclear Engineering

**MEASUREMENT OF HIGH VOLTAGE USING RUTHERFORD
BACKSCATTERING SPECTROMETRY**

A Thesis

by

CELESTINO PETE ABREGO

Submitted to the Office of Graduate Studies of
Texas A&M University
in partial fulfillment of the requirements for the degree of

MASTER OF SCIENCE

Approved by:

Chair of Committee, Ron Hart
Committee Members, Pavel Tsvetkov
David Church
Head of Department, William Burchill

December 2006

Major Subject: Nuclear Engineering

ABSTRACT

Measurement of High Voltage Using Rutherford Backscattering Spectrometry.

(December 2006)

Celestino Pete Abrego, B.S., Texas A&M University-Kingsville

Chair of Advisory Committee: Dr. Ron Hart

A novel variation of Rutherford Backscattering Spectrometry (RBS) has been utilized to measure a high voltage collected on an aluminum target by Direct Energy Conversion. The maximum high voltage on the target was measured to be 97.5 kV +/- 2 kV. The resistance of the circuit was then calculated based on the current driving different target voltages. The resistance was calculated to be $199.4\text{G}\Omega$ +/- 5%. It was shown that by simply measuring the neutral particles' energy spectra, the voltage on the target and resistance of the circuit can be found with certainty. The experimental data agree well with previous work and with the scattering theory developed. Thus, the capability of RBS has been extended to measure high voltages generated by direct energy conversion; this is something that has not been done before.

DEDICATION

To my wife

ACKNOWLEDGEMENTS

I would like to thank Dr. Hart for his guidance and for the curiosity he instilled during this research. I would also like to acknowledge previous researchers that made this thesis possible: Avery Bingham, Jesse Carter, and Lucas Phinney. I also thank Michael Martin who aided me during the experimental process. Lastly, I would like to thank Dr. Tsvetkov for his dedicated research in Direct Energy Conversion.

TABLE OF CONTENTS

	Page
ABSTRACT	iii
DEDICATION	iv
ACKNOWLEDGEMENTS	v
TABLE OF CONTENTS	vi
LIST OF FIGURES.....	viii
 CHAPTER	
I INTRODUCTION.....	1
II EXPERIMENTAL SYSTEM.....	5
Overview of Ion Accelerator.....	5
Target Chamber.....	7
Charge Collection Apparatus	9
III EXPERIMENTAL THEORY	11
Overview	11
Rutherford Backscattering Spectrometry	11
Kinematic Factor	13
Scattering Dynamics	15
Deflection Apparatus.....	17
IV PROCEDURE	21
Calibration.....	21
High Voltage Experiment.....	22
V RESULTS AND DISCUSSION.....	24
Calibration.....	24
High Voltage Experiment.....	26
VI CONCLUSIONS.....	30

	Page
REFERENCES	31
APPENDIX I	32
APPENDIX II	35
VITA	36

LIST OF FIGURES

	Page
Figure 1. Test facility for the FFMCR prototype.	2
Figure 2. Accelerator system.	5
Figure 3. Target chamber.	7
Figure 4. Suppression grid.	8
Figure 5. Charge-collection apparatus.	10
Figure 6. Elastic two-body collision.	14
Figure 7. Scattering theory.	17
Figure 8. Deflection apparatus.	18
Figure 9. Total deflection as a function of voltage.	20
Figure 10. Target current as a function of mesh voltage.	22
Figure 11. Calibration backscattering spectra.	24
Figure 12. Linear energy scale of MCA.	25
Figure 13. Neutral particle spectra.	27
Figure 14. Experimental results.	28
Figure 15. Resistance determined with RBS.	29
Figure 16. Dimensions of deflection apparatus.	35

CHAPTER I

INTRODUCTION

The United States Department of Energy's Nuclear Energy Research Initiative (NERI) project identified the fission fragment magnetic collimator reactor (FFMCR) as a concept to offer great promise. Consequently the NERI project, in conjunction with Texas A&M University, through Sandia National Laboratories, funded experimental verification of the basic principles behind the FFMCR concept and served as the motivation for this research.

The goal of Texas A&M University has been to develop and characterize a FFMCR collector prototype. The governing principle behind the collection process is known as direct energy conversion (DEC). Direct energy conversion is the process of converting the kinetic energy of charged particles, especially those released in nuclear reactions, to electric potential energy by decelerating and collecting the particles on high-voltage plates.¹⁾ The Texas A&M University prototype will utilize the K500 superconducting cyclotron to direct a beam of singly charged helium ions to the collector of the prototype which is predicted to achieve electric potentials as high as 1MV.

The K500 Cyclotron Facility has the Superconducting Solenoid Rare-Isotope Beam Line with a large-bore high-field superconducting solenoid called BigSol. The K500 is typically used for production, separation, and focusing of rare isotopes for nuclear reaction and nuclear structure studies. Particles emitted in the range ~1-6

This thesis follows the *Journal of Nuclear Science and Technology*.

degrees enter the solenoid and are focused approximately 4-meters beyond at the intermediate focus. Groups of particles may be selected using a circular aperture. The particles are transported through a 7-meter line to the Final Focus with a quadrupole triplet. This line has been selected for use in experiments with the scaled FFMCR prototype.²⁾ The BigSol line, BigSol 7 Tesla superconducting magnet and other line components are also shown in Figure 1.

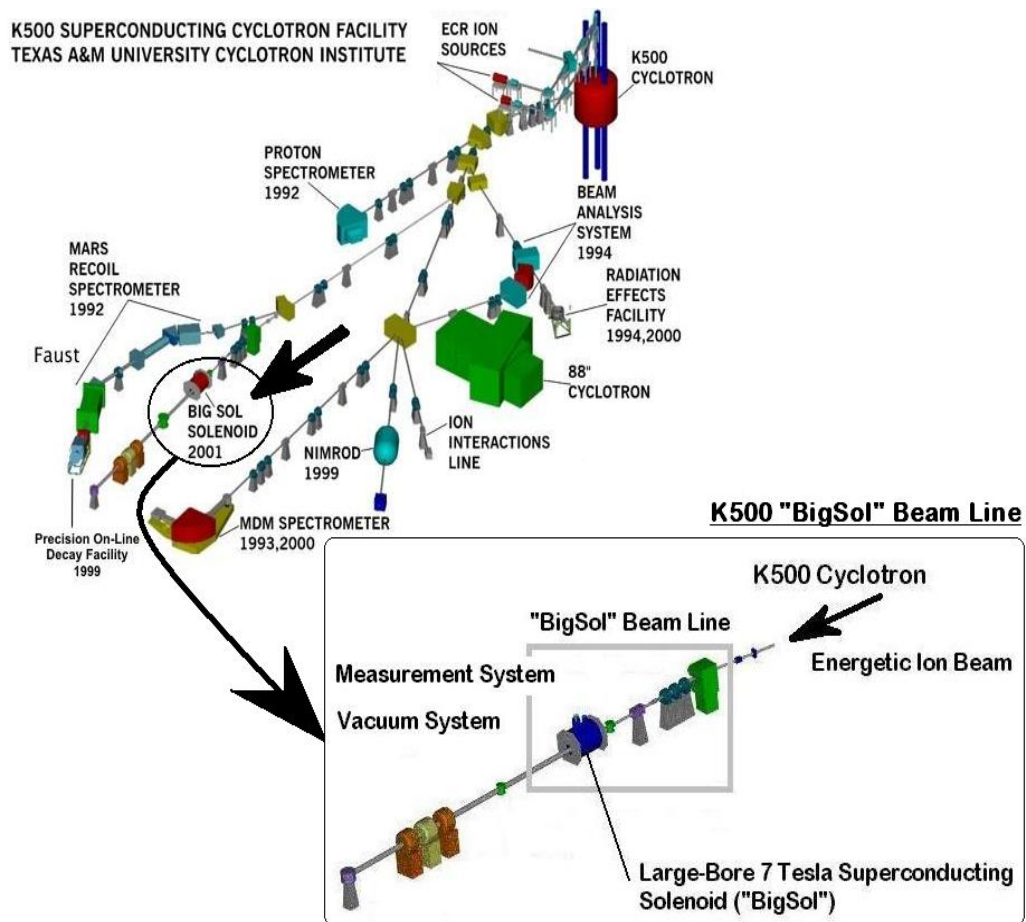


Figure 1. Test facility for the FFMCR prototype.

The present work is focused on a geometrically scaled model of the FFMCR prototype using a 150 kV accelerator ion beam in the Texas A&M University Ion Beam Laboratory.

The DEC concept utilizing the kinetic energy of Fission Fragments (FFs) was originally proposed by E.P. Wigner in 1944²⁻³⁾. Early work validated the basic physics behind DEC; however, technological constraints limited the achieved efficiencies. Because of the performance challenges faced by early prototypes, most of DEC research ceased by the late 1960's.²⁾ More recent studies have been done by Barr and Moir at Lawrence Livermore National Laboratory, and at the Texas A&M University Ion Beam Laboratory. These investigations were accomplished by bombarding a target with a mono-energetic ion beam, thus collecting the charged particles on to a single stage collection plate. This phenomenon is a basic principle of DEC and is essential for directly converting the energy of FFs into electricity. Although FFs are typically liberated with large distributions in angle and energy, these experiments were concerned with physical aspects of achieving large voltages; therefore, the use of a mono-energetic ion beam is valid.

Among the physical engineering challenges for this project, proper insulation of the target and accurate resistor characterization have both proven to be essential. Barr and Moir reported achieving voltages of 100 kV; however, collection efficiency was less than 60%.⁴⁾ The most recent work done at Texas A&M University achieved excellent results; voltages of 150 kV were produced with an efficiency of approximately 92%.²⁾ This is a substantial improvement from previous work where a voltage of 40 kV and

approximately 90% efficiency were reported.⁵⁾ Factors contributing to this improved performance include modification of the following system components: insulating material, resistors, and target holder apparatus. The previous work done at Texas A&M University relied on a plateau of current method for determining the voltage achieved on the collection plate or target.⁶⁾ The plateau method has proven to work well if there are no physical complications such as non-linear resistor response and electric breakdown of the insulating apparatus. In the case where a resistor may be faulty, it can become difficult to maximize target voltages and efficiency with consistency and accuracy. Furthermore, it becomes increasingly difficult if the non-linear resistor response is coupled with electric breakdown through the insulating apparatus. As a result of these physical issues a variation of Rutherford Backscattering Spectrometry has been employed to verify and validate results reported from Texas A&M University.

CHAPTER II

EXPERIMENTAL SYSTEM

Overview of Ion Accelerator

A linear accelerator capable of producing ions with energies up to 150 keV was used during this research. The ions used in this experiment were singly charged helium atoms. This section will give a brief overview of the mechanisms responsible for producing an ion beam. Refer to Figure 2 for a schematic of the linear accelerator.

- | | |
|---|---------------------------------------|
| A Physicon Ion Source | I First Collimator |
| B Acceleration Column | J Sweep Plates |
| C Electron Backstreaming Barrier | K Ion Pump |
| D Vertical and Horizontal Deflection Plate Assembly | L Horizontal and Vertical Collimators |
| E Glass Cross Shutter | M Liquid Nitrogen Cold Trap |
| F Glass Cross | N Beam Profile Monitor |
| G Diffusion Pump | O Target Chamber Collimator |
| H Separator Magnet | P Target Chamber |

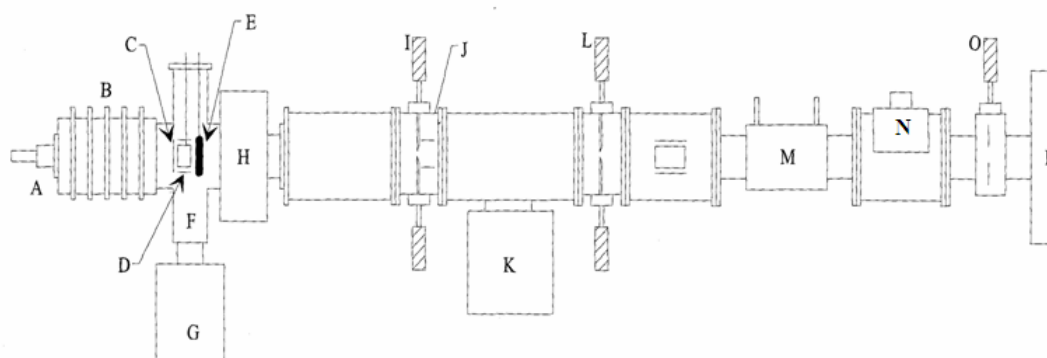


Figure 2.Accelerator system.⁶⁾

Gas atoms are fed in to the Physicon hot cathode ion source where they become ionized. The ions are accelerated and formed into the beam by the ion-extractor-

electrode system. The ion beam then leaves the extractor and passes through the focusing lens electrodes. After leaving the accelerating column, the ions enter a glass cross region. Inside the glass cross are a few instruments for modifying the ion beam. There is a shutter to stop the beam and measure the beam current at this point. Also, there is a set of vertical deflection plates that operate at voltages between 0-200 V. The deflection plates are used to adjust the vertical height of the beam. Connected to the bottom of the glass cross is a 6-inch Varian diffusion pump. When the beam is not in use this pump maintains a pressure of approximately 8×10^{-7} torr in the glass cross, and 2×10^{-6} torr during operation of the beam.

Next, the ion beam enters a magnetic field generated by the separation magnetic. The magnetic field is adjusted to separate and direct the desired ions into the target chamber where it will collide with the target. After mass separation the ion beam enters the beam line, which is maintained in the 10^{-8} Torr range by an ion pump. Low gas pressure minimizes collisions that the beam has with other atoms, thereby minimizing the probability that the ions in the beam become neutralized. Knife edge collimators are also present in the beam line and are used to shape the beam. A liquid nitrogen cold trap is also used at the end of the beam line and is particularly useful for condensing atoms such as water molecules and impurities such as vacuum pump oil; this prevents them from entering the target chamber. Finally, at the entrance to the target chamber there is an adjustable beam collimator at the end of the beam line. This is the last instrument to shape the beam before it enters the target chamber and may be used to adjust the beam diameter to 1/4", 1/8", and 1/32".

Target Chamber

The target chamber is maintained on the order of 5×10^{-8} Torr during operation by a diffusion pump and a cryopump. Refer to Figure 3 for a schematic of the target chamber. Before the beam enters the target chamber the current is measured on the shutter, which may be opened or closed.

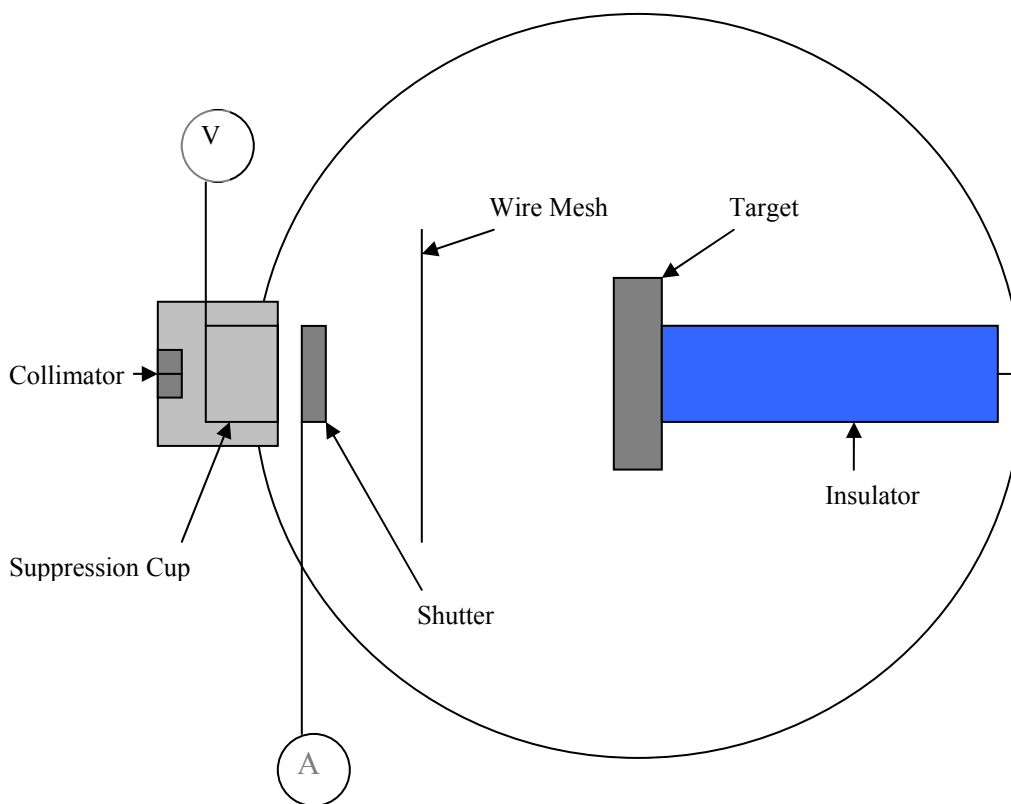


Figure 3.Target chamber.

An accurate measurement of the beam current before it strikes the target is essential for this work. The implementation of a bias cup before the shutter has proven to be particularly useful to achieve accurate current measurements. When the beam strikes the shutter secondary electrons are produced. This phenomenon increases the value of the current measured by the electrometer at the shutter by approximately 100%. By utilizing the bias cup the electrons are suppressed and kept on the shutter, thereby allowing an accurate measurement of the beam current. Recent experiments have shown the bias cup to be most effective when -200 V is applied, therefore -200 volts was applied during the present work.

Finally, inside the target chamber is a 76% transmission electron suppression grid, see Figure 4.

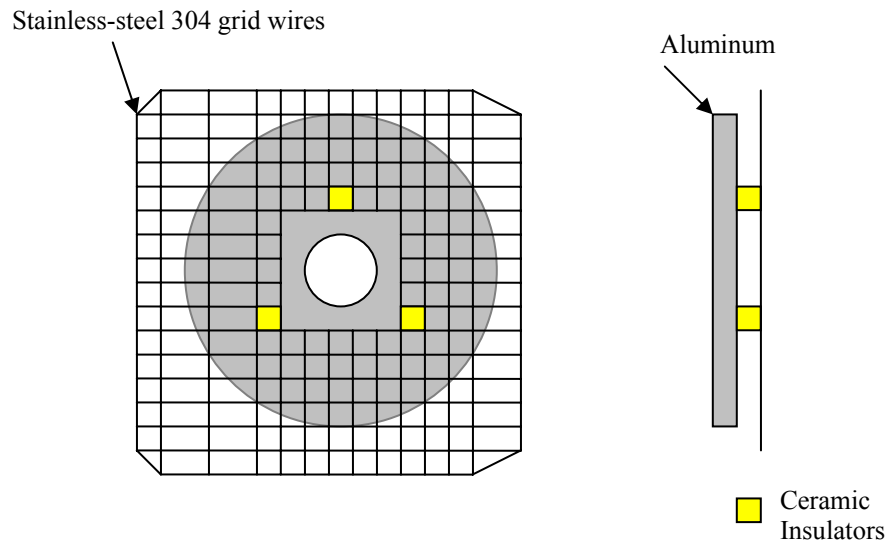


Figure 4.Suppression grid.

The plane of the grid is perpendicular to the ion beam direction, and the beam travels through the center of the grid. There is a 1-inch diameter opening in the grid to allow the ion beam to travel through it without collisions with the stainless-steel 304 grid wires, see Figure 4. A positive or negative bias can be applied to the mesh to suppress secondary electrons created in the chamber wall near the mesh.

Charge Collection Apparatus

Charge was collected on a cylindrical aluminum disk, or target, and has a diameter of 2.5 inches and 0.5 inches thick. The target is insulated from ground with Nylatron Blue Nylon. Holes are drilled in the Blue Nylon to hold the resistors in place; the resistors must be spaced such that the potential difference between any two points is minimized⁷⁾. This is done to prevent electrical breakdown across the vacuum. The resistors used in this experiment are 100 G Ω +/-5% at 90 kV high voltage resistors manufactured by Nichrome Electronics Incorporated. The target is connected and secured to the resistors by a solid wire. For this research two 100G Ω resistors were used in series for an effective resistance of 200G Ω . Previous work done in the Ion Beam Laboratory at Texas A&M University has shown these particular resistors have a constant resistance. See Figure 5 for a photograph of the charge-collection apparatus.

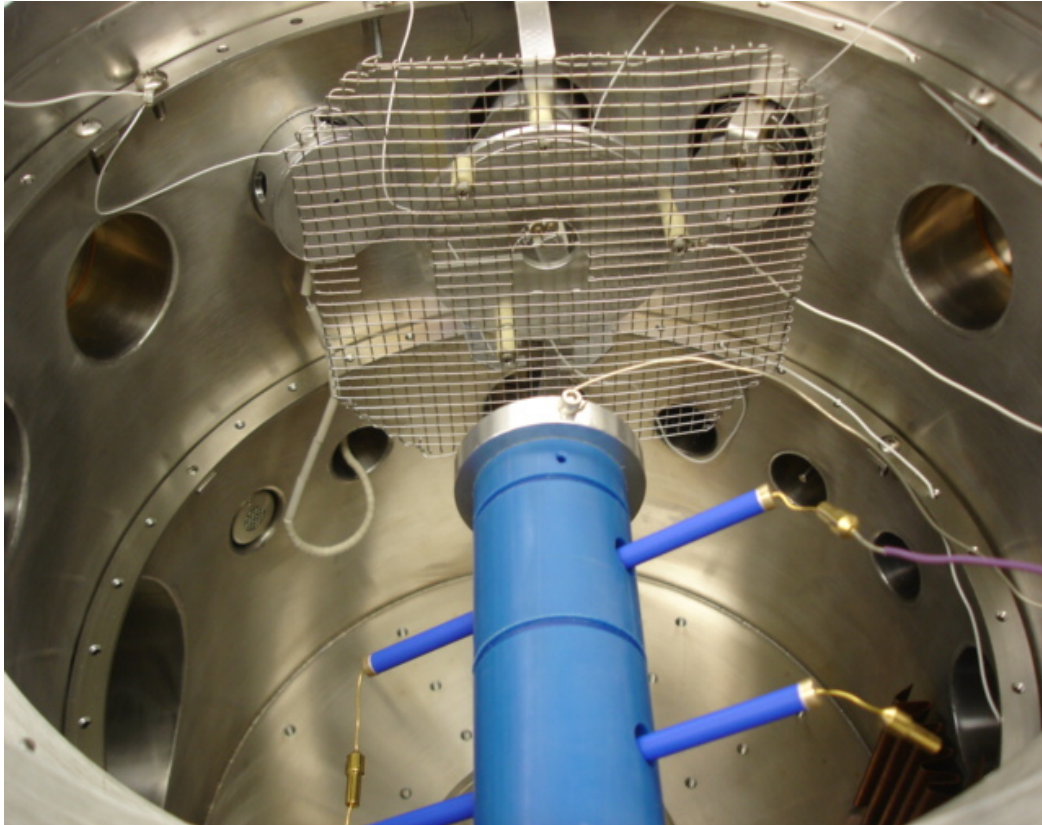


Figure 5.Charge-collection apparatus.

CHAPTER III

EXPERIMENTAL THEORY

Overview

The method of Rutherford Backscattering Spectrometry (RBS) has been utilized to provide an additional method to verify and validate results determined at Texas A&M University. To achieve this goal, the typical RBS measurement technique has been modified to accommodate our particular objectives. This section will focus on describing the conventional methods of performing an RBS experiment. After an overview RBS is given, an explanation of how and why the technique has been modified will be given.

Rutherford Backscattering Spectrometry

In a typical RBS experiment, a beam of mono-energetic collimated ions impinges perpendicularly on a grounded target; ions interact with the target atoms and scatter backward into a detection system. The detected ions give information about the target composition and surface impurities. This experiment is not a typical RBS experiment; the purpose of this research is to determine the value of the voltage accumulated on the target by direct energy conversion.

There are four basic physical concepts introduced when performing RBS⁸⁾:

- Energy Transfer from the projectile to a target nucleus is an elastic classical two-body collision. This introduces the concept of the *kinematic factor* and provides the capability of mass perception.
- There exists a certain probability of a two-body collision occurring for a given combination of projectile and target atom. This introduces the concept of the *scattering cross section*, and provides the capability of quantitative analysis of atomic compositions.
- Average energy loss of an atom moving through a dense medium. This introduces the concept of the *stopping cross section*. This introduces the capability of depth perception.
- There is a statistical fluctuation in the energy loss of an atom moving through a dense medium. This process introduces the concept of *energy straggling* and limits the maximum mass and depth resolution of backscattering spectrometry.

This research will primarily rely on the concept of the kinematic factor to verify the high voltage produced on the target. The scattering cross section will provide a check to ensure that the relative counts detected by the multi-channel analyzer (MCA) follow the differential Rutherford scattering cross section, given by Equation 1.⁸⁾

$$\frac{d\sigma}{d\Omega} = \left(\frac{Z_1 Z_2 e^2}{4E} \right)^2 \frac{4}{\sin^4 \theta} \frac{[\sqrt{1 - ((M_1/M_2)\sin\theta)^2} + \cos\theta]^2}{\sqrt{1 - ((M_1/M_2)\sin\theta)^2}} \quad (1)$$

Equation 1 is the effective differential cross sectional area per steradian of a projectile with mass M_1 , atomic number Z_1 , and energy E , scattering off of a target atom with mass M_2 , atomic number Z_2 at an angle of θ . It should also be noted that e is given in cgs units therefore $e=4.80286 \times 10^{-10}$ statC, or converted to SI units $e=1.4398 \times 10^{-13}$ MeV-cm. In general the count rate is inversely proportional to the square of the incident projectile energy; therefore, decreasing the energy of the incident projectile by one half will increase the probability of scattering in to a particular angle by a factor of four.

For thin targets, approximately a few mono-layers, stopping cross sections will have little effect on the incident particle as it traverses the medium. Hence by scattering off a thin target, it may be assumed that the energy after a scattering event will be due to the kinematic factor described in the next section

Kinematic Factor

When a particle of mass M_1 , moving with constant velocity, collides elastically with a stationary particle of mass M_2 , energy will be transferred from the moving mass to the stationary particle. In the context of this analysis mass M_1 will be defined as the mass of the projectile, or ion in this case. M_2 will be defined as the target atom.

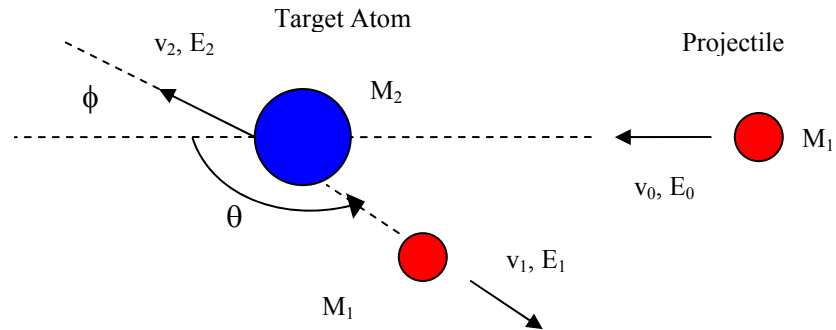


Figure 6.Elastic two-body collision.

Figure 6 is a representation of an elastic collision between a projectile with mass M_1 , with velocity v_0 , and energy E_0 and a target mass M_2 , which is initially at rest. After the collision, the projectile and the target mass have velocities and energies v_1 , E_1 , and v_2 , E_2 respectively. The angles θ and ϕ are positive as shown and all quantities refer to a laboratory reference frame. Two conditions must be met when assuming that the interaction between the two atoms can be properly described by a simple two-body collision⁸⁾:

- The energy of the projectile E_0 must be larger than the binding energy of the atoms in the target. Chemical bonds are on the order of 10 eV.
- Nuclear reactions and resonances must be avoided. Therefore an upper limit to the projectiles energy will be imposed. For He^+ ions, resonances appear at 2 to 3 MeV.

Assuming these conditions are met, the simple elastic collision of the two masses can be solved by applying conservation of energy and momentum. The ratio of the projectile

energy after the elastic collision to that before the collision is defined as the *kinematic factor* k , and is equal to equation 2.

$$k \equiv \frac{E_1}{E_0} \quad (2)$$

Applying conservation of momentum and conservation of energy to the situation shown in Figure 6, the kinematic factor can be found analytically and shown to be equal to equation 3.⁸⁾

$$k = \left\{ \frac{\left[(1 - (M_1/M_2)^2 \sin^2 \theta) \right]^{1/2} + (M_1/M_2) \cos \theta}{1 + (M_1/M_2)^2} \right\}^2 \quad (3)$$

The kinematic factor depends only on the ratio of the projectile to the target masses, and the scattering angle θ .

Scattering Dynamics

As mentioned the basis for the proposed measurement technique is RBS; however, a major difference lies between the two techniques. Classic RBS utilizes a grounded target during the measurement procedure, thus an electric voltage would never accumulate. This experiment is concerned with electric voltages developed on the target therefore; the target must not be grounded. When voltages are established and stabilized on the target interactions between the ions and the electric field produced by the target will occur. At target voltage equilibrium, energetic singly charged ions will approach

the target and begin to slow down due to their interaction with the electric-potential field produced by the voltage on the target. This slowing down process is the key point that will allow the determination of the target voltage. Upon impinging the target all ions will experience a decrease in energy due to the kinematic factor. Furthermore, a fraction of the ions will become neutralized and backscatter into the detection system. After the ion becomes neutral it will no longer be affected by the electric field as it approaches the detector, see equations 4, 5 and Figure 7. Thus the energy of the detected neutral particles, E_n , has an energy that is reduced by the potential field interaction and a specific kinematic factor. Moreover, the charged particle's energy, E_+ , has an increased value due as the charged particles are accelerated away.

$$E_n = (E_0 - qV)k \quad (4)$$

$$E_+ = (E_0 - qV)k + qV \quad (5)$$

Therefore, by measuring the energy of the back scattered neutral particle the voltage on the target may be accurately determined. Backscattered charged particles also offer information about the voltage accumulated on the target; however, the energy resolution of the detection system must be better than available to verify the voltage accumulated on the target.

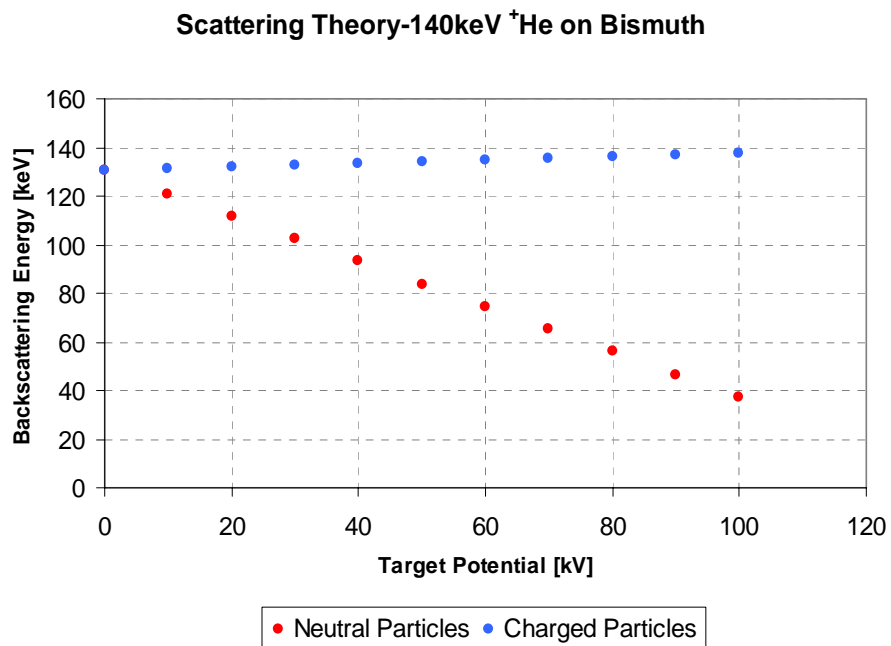


Figure 7.Scattering theory.

Thus, measuring the energy of the neutral particles to determine the voltage on the target was the focus of this research. To ensure that only neutral particles are detected, a system that deflects charged particles must be designed. This has been accomplished by the fabrication of a self-contained apparatus that houses a parallel plate system.

Deflection Apparatus

The fabrication of a deflection apparatus to deflect charged particles that scatter into the solid angle of the detector was an essential part of this research. Therefore a self contained apparatus that house the detector, parallel plates, and collimator was designed.

The deflection system was fabricated with tubular aluminum and was positioned inside one of the beam ports. To ensure a high vacuum was consistently maintained, pump out holes were also part of the apparatus design. Figure 8, shows a schematic of the deflection apparatus, along with the parameters of interest.

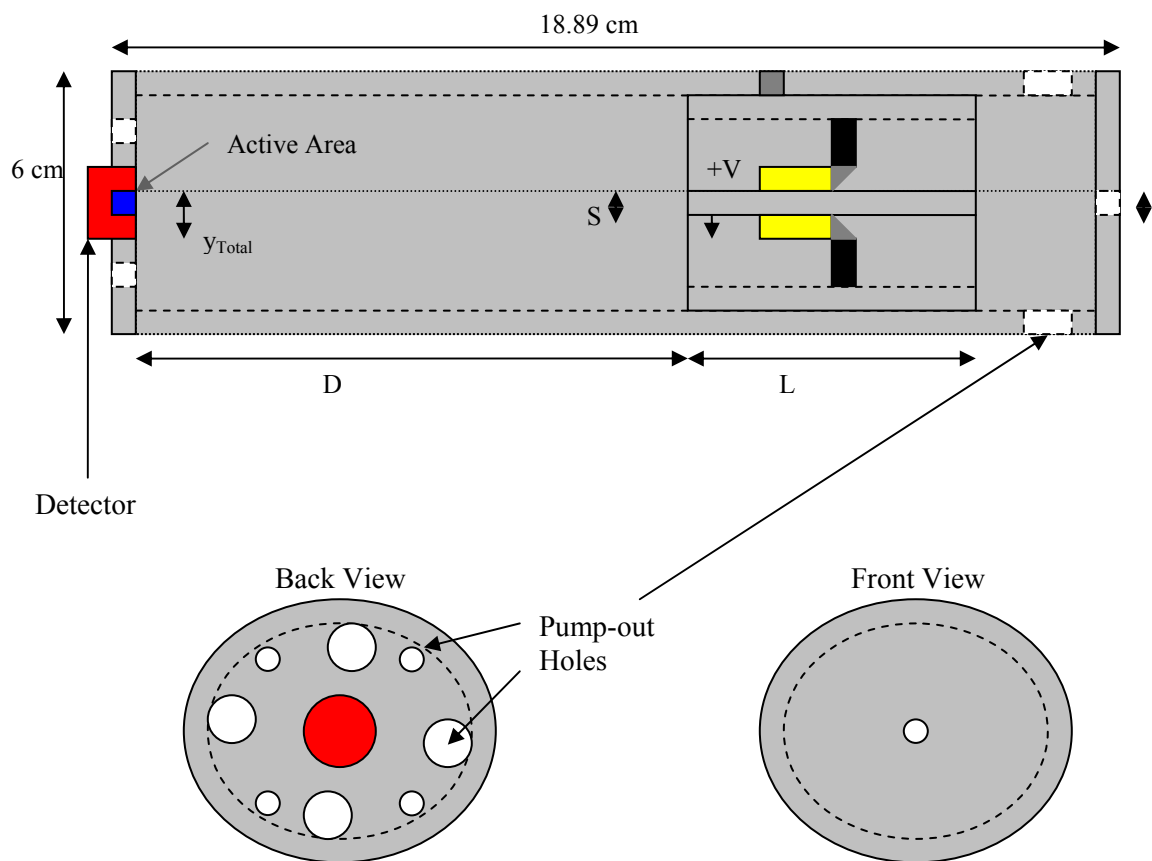


Figure 8. Deflection apparatus.

To determine the exact value of parameters such as: parallel plate spacing (S), length of parallel plates (L), distance from the end of the parallel plates to the detector (D), and parallel plate voltage (V), such that an ion with energy, E , would be deflected a total distance, y_{Total} , a model was developed. Classical physics was utilized to derive a

relationship between all of these parameters, the derivation can be found in Appendix I, and is shown to yield equation 6.

$$y_{\text{Total}} = \frac{qVL^2}{4SE} + \frac{qVDL}{2SE} \quad (6)$$

Plotting this equation, setting the parallel plate voltage as the independent variable, allowed the determination of the appropriate parallel plate voltage needed to deflect a charged particle away from the active area of the detector. It should also be noted that the voltage required to deflect all charged particles is not constant, Figure 7 illustrates this point. As the target voltage increase, so does the energy of the backscattered charged particles, thus the parallel plate voltage must increase with increasing target voltage. A plot of equation 6 is shown in Figure 9, with 140 keV as the value for E, other values are consistent with the final design and can be found in appendix II. This plot represents the maximum parallel plate voltage required to deflect charged particles away from the detector, since the active diameter of the detector is 5.64 mm, the maximum parallel plate voltage was approximately 1200V.

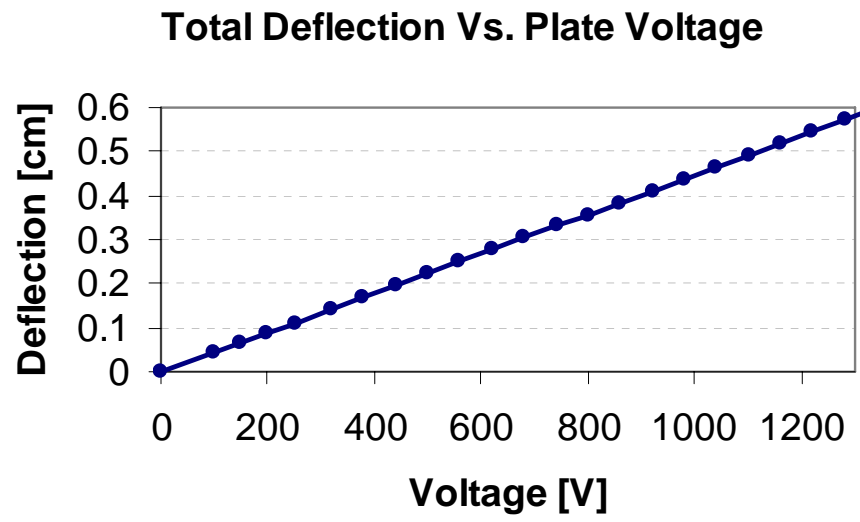


Figure 9. Total deflection as a function of voltage.

CHAPTER IV

PROCEDURE

Calibration

The RBS measurements carried out during this experiment rely on determining the relative energy shift of neutral backscattered particles. To achieve this goal a full scale energy calibration of MCA was essential. Earlier work done at Texas A&M University has shown that to effectively measure an energy shift using this variation of the RBS technique, a thin-film must be utilized. Therefore, it was chosen to attach a silicon substrate, which had been coated with approximately a mono-layer of bismuth, to the aluminum target.⁶⁾ Since bismuth is significantly heavier than silicon, scattering off it allowed a distinct energy peak to be visible; this is a very convenient observable in the spectrum and is extremely useful for both calibration measurements and high-voltage measurements.

For calibration purposes the target was grounded using a current integrator. Several backscatter spectra for helium ions were obtained by varying the incident energy from 70 keV to 140 keV, a total charge collection of approximately 2.25×10^{14} ions was observed during each of these measurements. Because of the concept of the kinematic factor, identification of the bismuth peak centroid channel allowed the determination of the energy of the backscattered ions.

To ensure that secondary electrons did not interfere with the total number of ions recorded by the current integrator, the mesh bias voltage that effectively suppresses all

secondary electrons was determined. Figure 10 shows the target current's dependence on mesh voltage. The plot shows that nearly all secondary electrons are suppressed at a mesh voltage of -350 V; therefore, a conservative value of -400 V was used during the calibration measurements.

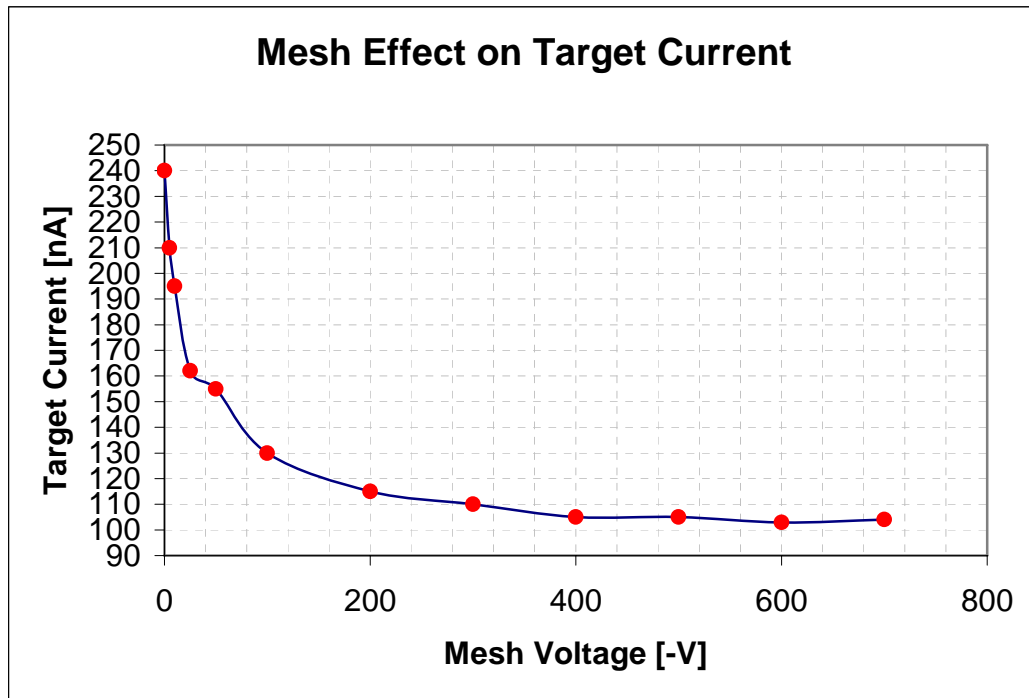


Figure 10. Target current as a function of mesh voltage.

After the energy scale of the MCA was determined, the target chamber was opened and resistors were attached to the target. During this time nothing else in the system was manipulated.

High Voltage Experiment

After the system reached acceptable vacuum conditions of approximately 5×10^{-8} torr, a 140 keV ion beam of singly charged helium atoms was developed to begin the

high-voltage experiment. Since previous work in the Ion Beam Laboratory at Texas A&M University has showed the current-voltage curve of these resistors to be very linear, it was expected that the voltages developed on the target would follow Ohm's law very closely⁵⁾. Therefore, 200G Ω of resistance will yield 100 kV of voltage on the target when the target current reaches 500 nA. Measurements of target voltages were taken at 100-500 nA, in 100 nA intervals. Since the neutral particles that scatter into the solid-angle of the detector are of greatest interests, the parallel plate voltage in the deflection apparatus was set to an appropriate value to ensure that all charged particles were deflected out of the solid angle of the detector. It should also be noted that there was no need for a bias on the mesh; once the target has a positive charge on it, secondary electrons were naturally suppressed. During the high-voltage measurements the target must reach a steady state or equilibrium before any data is taken. If equilibrium is not achieved, variation will be introduced into the backscattering spectra. The variation would occur during the time the ions are decelerating with the developing electric field, thus initial counts recorded in the MCA would skew latter counts and could introduce a source of error. Once the target has reached a steady state, the MCA software and the current integrator must be turned on simultaneously for the integrated current to truly represent the counts collected in the MCA. After 2.25×10^{14} ions were incident on the target, the shutter was closed and the current integrator was stopped simultaneously.

CHAPTER V

RESULTS AND DISCUSSION

Calibration

Based on previous work done with this variation of RBS, the position of the bismuth peak was expected to be near channel 1550 when a 140 keV helium ion backscatters into the solid angle of the detector. Upon analyzing the backscattered spectra, an additional peak was observed below the energy of the bismuth peak, see Figure 11.

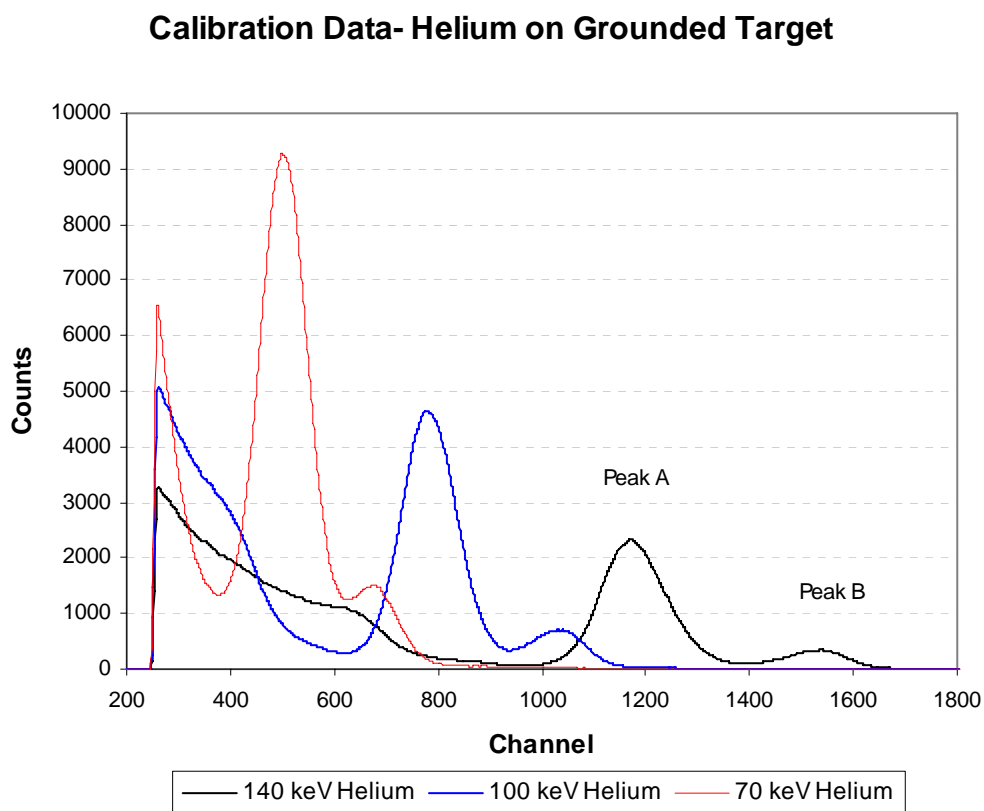


Figure 11. Calibration backscattering spectra.

This peak will be referred to as peak A, and the bismuth peak will be referred to as peak B during this analysis. Peak A shared a similar full width at half-max to peak B, yet the relative yield of peak A indicated about five times more surface atoms. An investigation into the kinematic factor of peak A was accomplished by varying the energy of incident helium ions incident on the target. It was concluded that the atomic mass of peak A was approximately 50 ± 3 atomic units, identifying it as vanadium. Since peak A is thin it was also be used an observable in the spectrum. The results of the calibration are shown in Figure 12. As expected the energy scale of the MCA is extremely linear with $.0765$ [keV/channel] and a zero off-set of 11.89 keV.

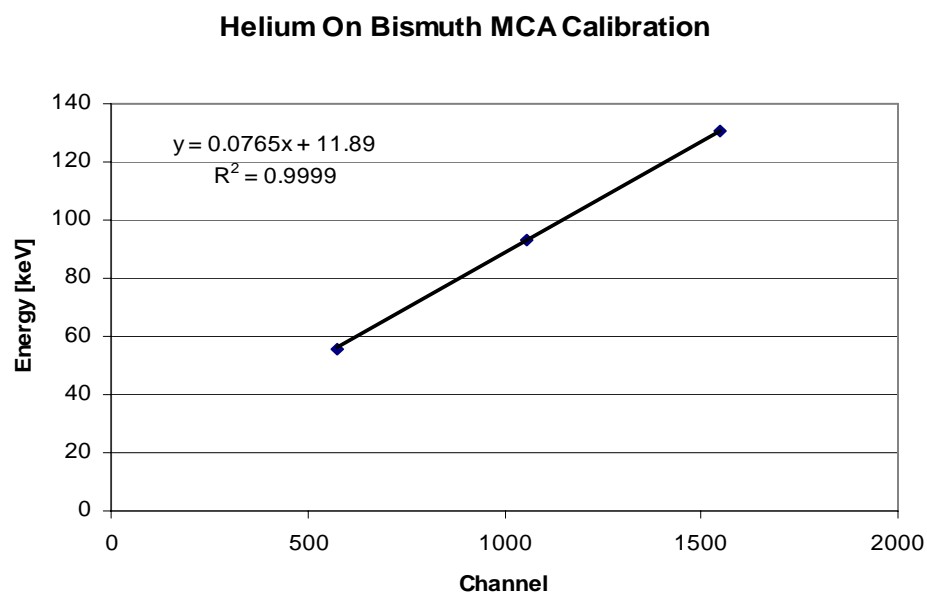


Figure 12.Linear energy scale of MCA.

High Voltage Experiment

The neutral particle spectra for 100-500 nA beam currents are shown in Figure 13. As the current bombarding the target increased, the measured energy of the neutral particle decreased as predicted in equation 4. It should also be noticed that the kinematic factors of layer A and layer B are such that the energy of the backscattering neutral particles actually begin to approach each other as the voltage on the target increases. This leads to some uncertainty with the actual centroid of peak B. Because of the uncertainty associated with the centroid position of the overlapping peaks, the MCA software utilized a peak search subroutine to minimize any error that may have been introduced. The peak search subroutine finds peaks using a rate of change of slope algorithm and sets regions of interest (ROI) around such areas. In these cases, the peak centroid of each ROI is calculated as a weighted average with the background or “tail” of the neighboring peaks subtracted out. Therefore, each peak is resolved separately and the centroid position of the peak is then determined.

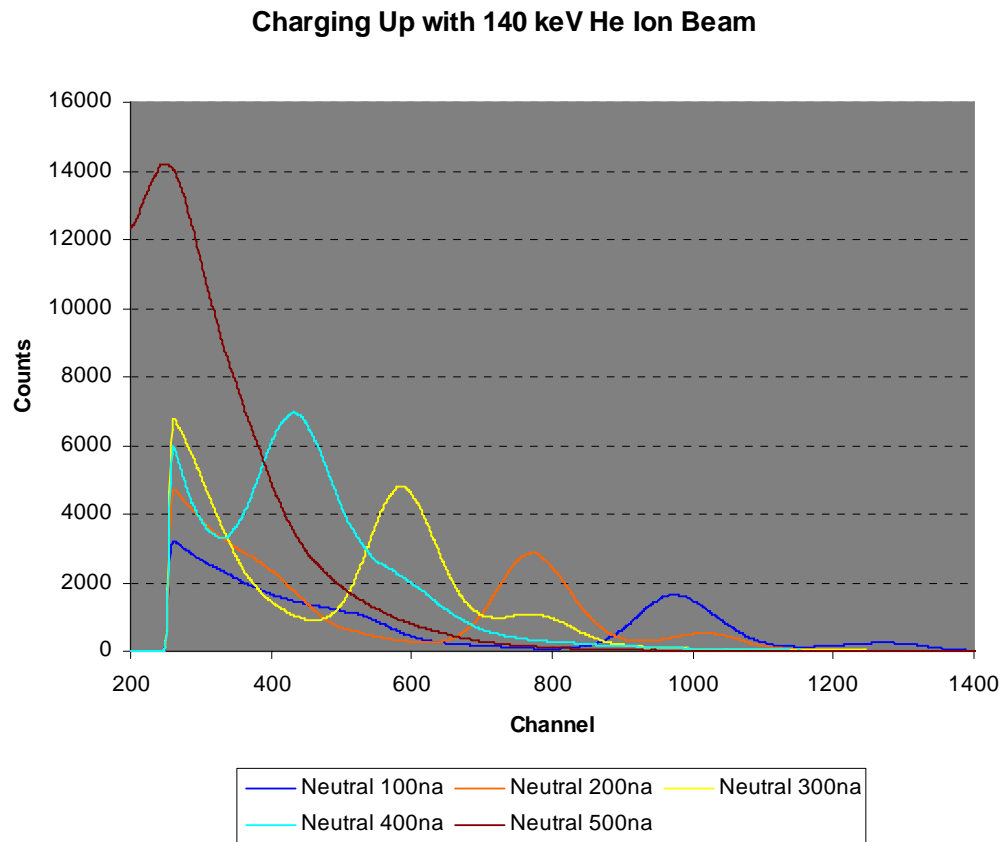


Figure 13.Neutral particle spectra.

After the measurements of the neutral particle spectra were accomplished, the centroid channel of each peak was converted to energy using the energy calibration developed in Figure 12. The energy of the neutral particles was then used in equation 4 to solve for the voltage on the Target.

Figure 14 is a plot of the neutral particle energy as a function of target voltage based on the experimental data. The results agree extremely well with the values predicted in the theory section. Since the target potential has been experimentally determined, the resistance through the circuit may be determined.

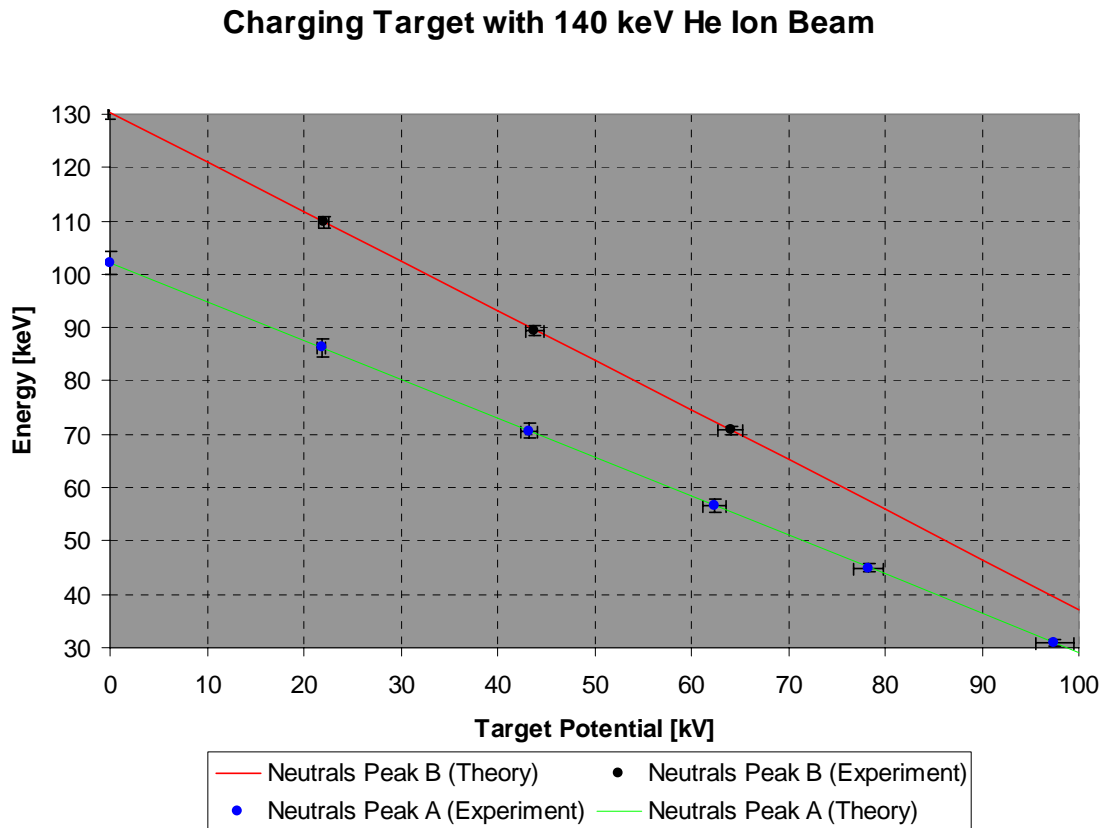


Figure 14. Experimental results.

Figure 15 is a plot of the target voltage, determined with RBS, as a function of current. Assuming Ohm's Law is valid, the resistance may be found by determining the slope of a linear trend line. The resistance determined from previous work, using the plateau method⁵⁾, agrees very closely (<1% difference) to the resistance determined from the data analyzed from peak A. Peak B is relatively close; however, because of uncertainties with centroid positions and fewer identifiable data points the resistance determined from peak B showed approximately 7% difference from previous work. A summary of the results are shown in Table 1.

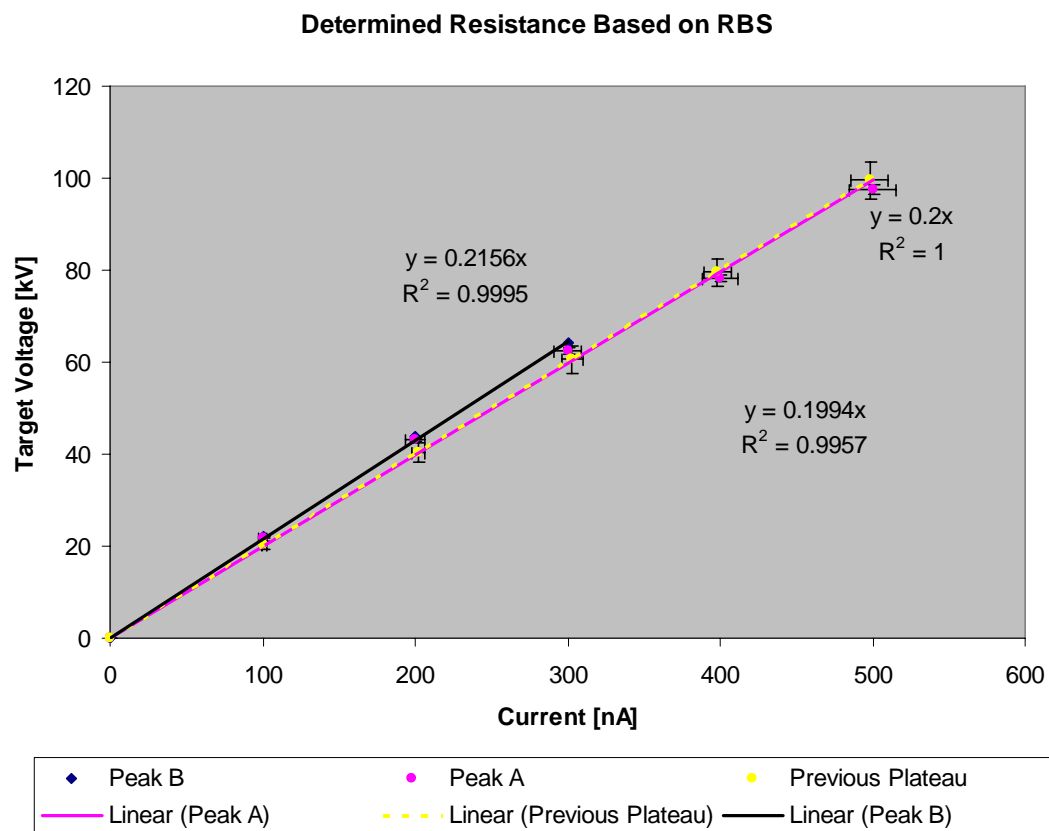


Figure 15.Resistance determined with RBS.

Table 1.Resistance determined with RBS.

	Peak A	Peak B	Previous Work
Resistance [GΩ]	199.4+/-10	215.6+/-11	200+/-6

CHAPTER VI

CONCLUSIONS

A novel variation of Rutherford Backscattering Spectrometry has been utilized to measure a high voltage collected on an aluminum target by DEC. A deflection apparatus was successfully designed and fabricated to prevent charged particles from entering the solid angle of the detector; this allowed the measurement of the neutral particle's backscattering spectra. The voltage applied to the parallel plates corresponded with theoretical values derived, and varied from 1000V to 1200V. The maximum high voltage on the target was measured to be 97.5 kV +/- 2 kV. The resistance of the circuit was then calculated based on the current driving different target voltages. The resistance was found to be 199.4 G Ω +/- 5%, this value closely agrees with previous work and the expected value of 200 G Ω +/- 5%, as advertised by Nichrome. The use of a silicon substrate coated with thin layers of atoms, proved to be a convenient target.

In conclusion, this thesis has successfully developed an alternate and unique measurement technique for determining high voltages accumulated by DEC. It was shown that by simply measuring the neutral particles energy spectra, the voltage on the target and resistance of the circuit can be found with certainty. The experimental data agrees excellently with previous work and with the scattering theory developed. Thus, the capability of RBS has been extended to measure high voltages generated by DEC; this is something that has never been done before. Future work should include an investigation into the charged particle phenomena described in the theory section as well as variations of the Rutherford scattering cross-section under these conditions.

REFERENCES

- 1) G.H. Miley, *Fusion Energy Conversion*, American Nuclear Society, Hinsdale, IL. (1976)
- 2) R. Hart, P. Tsvetkov, J. Carter, C. Abrego, A. Bingham, and L. Phinney, *Year Three Studies on the Modeling, Design, and Testing of the Scaled System Prototypes of Fission Fragment Magnetic Collimator Reactors*, Report Texas A&M University, College Station. (2006)
- 3) P.V. Tsvetkov, R. Hart, T. A. Parish, “Highly Efficient Power System Based on Direct Fission Fragment Energy Conversion Utilizing Magnetic Collimation”, *Proceedings of the 11th International Conference on Nuclear Engineering*, Tokyo, Japan, American Society of Mechanical Engineers. (2003)
- 4) W.L. Barr, R.W. Moir, “Test Results On Plasma Direct Converters,” *Nuclear Technology/Fusion*, **3**, 98. (1983)
- 5) K. Thompson, *Characterization of a Pulsed Beam Time-of-Flight System for Medium Energy He⁺ and C⁺ Backscattering Spectrometry*. M.S. Thesis, Texas A&M University, College Station. (1994)
- 6) J. Carter, *Analysis of a Direct Energy Conversion System Using Medium Energy Helium Ions*. M.S. Thesis, Texas A&M University, College Station. (2006)
- 7) R. Latham, *High Voltage Vacuum Insulation Basic Concepts and Technological Practice*, Academic, San Diego, CA. (1995)
- 8) W. Chu, J. Mayer, M. Nicolet, *Backscattering Spectrometry*, Academic Press, New York. (1978)

APPENDIX I

DERIVATION OF TOTAL DEFLECTION

A derivation of the total deflection experienced by the ions passing through the parallel plate system is presented. The problem will be broken into two parts and each part will be solved separately. After the two parts have been solved, they will be combined to give the final solution.

Qualitatively it can be understood that the total deflection will be due to a contribution, Δy_{pp} , from the force applied on the ion by the electric field of the parallel plates, plus deflection after the parallel plates due to the velocity gained as it traversed the parallel plates, $\Delta y_{a=0}$. The subscript $a=0$ is given because after the ion leaves the parallel plates acceleration experienced by the ion is zero. Therefore, the problem may be separated into two parts. Thus, the total deflection is given as Equation 7.

$$\Delta y_{\text{Total}} = \Delta y_{\text{PP}} + \Delta y_{a=0} \quad (7)$$

First, an expression will be found for the deflection of the ion as it passes through the parallel plates Δy_{pp} . Assuming constant acceleration, and recognizing that the velocity in the y-direction is initially zero, Equation 8 is given.

$$\Delta y_{\text{pp}} = \frac{1}{2} a_y t^2 \quad (8)$$

In this equation a_y is the constant acceleration experienced by the ion and t is the time spent under acceleration. Therefore, finding the acceleration and the time spent

accelerating will solve the first part of this equation. Solving for these terms is strait forward.

To solve for the acceleration recognize the only force acting on the ion is force of the electric field, qV/S , where S is the spacing of the parallel plates. Thus, the acceleration is solved for in Equation 9.

$$F=ma_y = \frac{qV}{S} \Rightarrow a_y = \frac{qV}{mS} \quad (9)$$

To solve for the time spent accelerating consider the length of the parallel plates, L , divided by the speed of the ion, V , and m is the mass of the ion, see Equation 10.

$$t = \frac{L}{v} = \frac{L}{\sqrt{\frac{2E}{m}}} \quad (10)$$

Using Equations 9 and 10 into equation 8 will give Equation 11.

$$\Delta y_{pp} = \frac{qVL^2}{4ST} \quad (11)$$

Now an expression for $\Delta y_{a=0}$ will be found. Recognizing acceleration is zero after the parallel plates and deflection is due to the velocity gained, V_{0y} , during the time the ion traversed the parallel plates Equation 12 gives the most simple solution for $\Delta y_{a=0}$.

$$\Delta y_{a=0} = v_{0y} T \quad (12)$$

Now the time, T , spent between the parallel plates and the detector becomes important.

To solve for the velocity gained equation 13 is given.

$$v_{0y} = a_y t = \left(\frac{qV}{mS} \right) \frac{L}{\sqrt{\frac{2E}{m}}} \quad (13)$$

To solve for T we must consider the distance, D, between the parallel plates and the detector. Very similar to Equation 10, the time is found in Equation 14.

$$T = \frac{D}{\sqrt{\frac{2E}{m}}} \quad (14)$$

Combining equations 12, 13, and 14, the deflection after the parallel plates is found and given in Equation 15.

$$\Delta y_{a=0} = \frac{qVLD}{2SE} \quad (15)$$

Finally, the Equations 15 and 11 may be substituted in to Equation 7 to given the expression for the total deflection experienced by the ion, Equation 6.

$$\Delta y_{\text{Total}} = \frac{qVL^2}{4SE} + \frac{qVDL}{2SE} \quad (6)$$

APPENDIX II
DIMENSIONS OF DEFLECTION APPARATUS

Figure 16 shows the final dimensions used for the deflection apparatus fabricated.

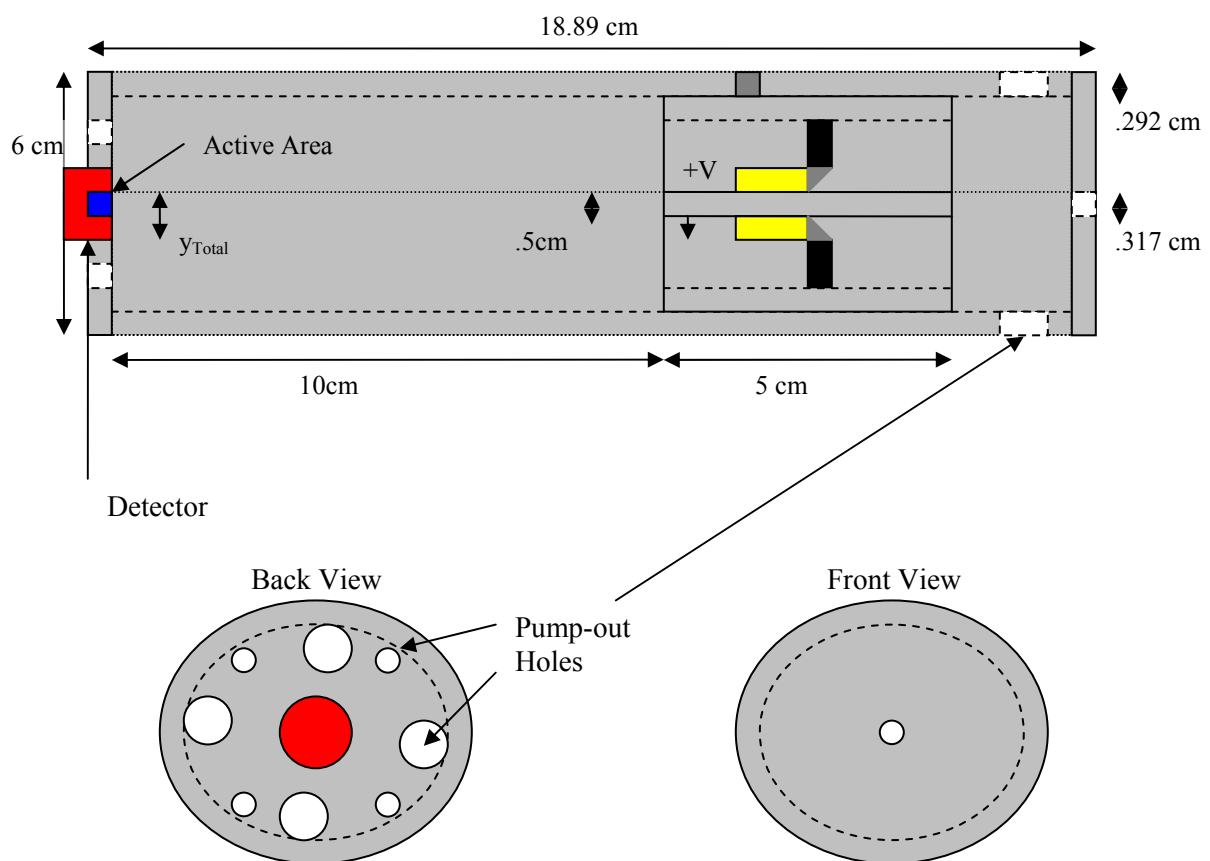


Figure 16.Dimensions of deflection apparatus.

VITA

Celestino Pete Abrego was born in Corpus Christi, Texas. In December 2004, he received a Bachelor's Degree in physics from Texas A&M University-Kingsville.

While attending Texas A&M-Kingsville, he was admitted into the Sigma Pi Sigma honor society. After receiving his physics degree, he studied nuclear engineering at Texas A&M University. He received his Master of Science in nuclear engineering in December 2006. He may be contacted through email, at cabrego@ne.tamu.edu.